Journal of Colloid and Interface Science 335 (2009) 250–256

Contents lists available at ScienceDirect

Journal of Colloid and Interface Science

www.elsevier.com/locate/jcis

Electrokinetics of suspended charged particles taking into account the excluded volume effect

M.J. Aranda-Rascón [a], C. Grosse [b,c], J.J. López-García [a], J. Horno [a,*]

[a] Departamento de Física, Universidad de Jaén, Campus Las Lagunillas, Ed. A-3, 23071 Jaén, Spain
[b] Departamento de Física, Universidad Nacional de Tucumán, Av. Independencia 1800, 4000 San Miguel de Tucumán, Argentina
[c] Consejo Nacional de Investigaciones Científicas y Técnicas, Argentina

ARTICLE INFO

Article history:
Received 20 December 2008
Accepted 23 February 2009
Available online 7 April 2009

Keywords:
Excluded volume effect
Finite ion size
Electrophoretic mobility
Conductivity increment

ABSTRACT

In two recent works [López-García et al., J. Colloid Interface Sci. 316 (2007) 196; López-García et al., J. Colloid Interface Sci. 323 (2008) 146] we presented a simple modification of the standard electrokinetic model that takes into account the finite size of ions in the electrolyte solution. In the first we presented numerical results for the equilibrium properties while, in the second, we calculated the effect of the excluded ion volume on the electrophoretic mobility. In the present work we first extend our previous results incorporating a distance of closest approach of the ions to the particle surface. We then calculate the conductivity increment and present a detailed interpretation of the mobility and conductivity increment results, based on the analysis of the equilibrium and field-induced ion concentrations and of the convective fluid flow in the neighborhood of the particle surface. We show that the inclusion of the ion size effect generally improves the predictions of the standard electrokinetic model: both the electrophoretic mobility and the conductivity increment increase. We also show that, largely due to the above-noted extension of considering a minimum approach distance between the ions and the particle surface, the excluded volume effect is not negligible even for weakly charged particles.

1. Introduction

The classical description of colloidal suspensions is based on a series of assumptions that constitute the standard electrokinetic model: suspended particles are surrounded by a perfectly smooth uniform surface density of fixed charge, ions can be treated as mathematical points, and the macroscopic permittivity and viscosity values remain valid at the microscopic scale up to the very surface of the particle. With these assumptions, the equilibrium ion density coincides with the Gouy-Chapman distribution, the surface conductivity coincides with the conductivity of the diffuse double layer, and the ζ potential coincides with the equilibrium surface potential.

Despite its almost universal use, the classical model fails to predict crucial experimental trends: ζ potential values calculated from experimental electrophoretic mobility, conductivity increment, and permittivity increment data using this model usually do not coincide with one another [1–6]. The most common way to address these difficulties is to consider that the surface of the particle is more complex than assumed by the model: it is either surrounded by a thin layer where the ion density is determined by adsorption isotherms or the particle surface is rough or hairy so that both fixed charges and free ions populate the surface layer [7–12]. Although these generalizations solve some deficiencies of the classical model [13], they usually worsen the interpretation of experimental data for high electrophoretic mobilities [14]. Furthermore, they address surface properties that are specific to each particular particle–electrolyte solution combination, so that they include a series of adjustable parameters.

In this and in our two previous works [15,16], we address a different shortcoming of the standard electrokinetic model: ions in the electrolyte solution actually have a finite size. While the way in which this finite size is incorporated into the equations may vary [17,18], the corresponding correction is universal since it does not depend on any particle property. Therefore, the ion size should be characterized by parameters that are not adjustable.

Although previous works dealing with the finite ion size exist [19,20], they are limited to the equilibrium solution of the Poisson–Boltzmann equation with plane geometry. In [15] we presented numerical results for the equilibrium properties and spherical geometry while, in [16], we calculated the effect of the excluded ion volume on the electrophoretic mobility. In the present work we first extend our previous results taking into account that the ion size not only establishes a minimum distance between ions but also determines a minimum distance between an ion and the surface of the particle. We then calculate the conductivity increment and present a detailed interpretation of the mobility

* Corresponding author. Fax: +34 953 212838.
E-mail address: jhorno@ujaen.es (J. Horno).

0021-9797/$ - see front matter © 2009 Elsevier Inc. All rights reserved.
doi:10.1016/j.jcis.2009.02.057

and conductivity increment results, based on the analysis of the equilibrium and field-induced ion concentrations, and of the convective fluid flow in the neighborhood of the particle surface.

We show that the inclusion of the excluded volume effect generally improves the predictions of the standard electrokinetic model: both the electrophoretic mobility and the conductivity increment increase. We also show that, because of the above-noted extension that incorporates a distance of closest approach of ions to the particle surface and to ion convection, the ion size effect is not negligible even for weakly charged particles.

2. Theoretical model

Let us to consider a spherical particle of radius a immersed in an infinite electrolyte solution with m ionic species. The equations governing the steady state dynamics of this system are well known:

(a) Nernst–Planck equations for the ionic fluxes,
(b) Continuity equations for each ionic species,
(c) Poisson equation for the electric potential,
(d) Navier–Stokes equation for a viscous fluid, and
(e) Continuity equation for an incompressible fluid.

For a hypothetic ideal electrolyte solution, this set of equations, together with the appropriate boundary conditions, constitutes the standard electrokinetic model [1–6]. In order to treat nonideal solutions, the effect of the ion size constraints on the dynamics of the system should be taken into account. If the electrolyte solution does not behave ideally and the ions are assumed to have a finite size, the density determined after subtracting the ion volume is higher than the density determined assuming that ions behave as point charges. This concentration difference modifies the ion flows by increasing the concentration gradients. The ion volume also decreases the diffusion coefficient by decreasing the mean free path. Due to these two competing effects a correction factor γ_i is introduced as a modifier of the diffusive term in the Nernst–Planck equations for the ion flows ("steric hindrance" effect [21]),

$$c_i(\vec{r})\vec{v}_i(\vec{r}) = -D_i c_i(\vec{r})\nabla\left\{\ln[\gamma_i c_i(\vec{r})] + \frac{z_i e}{kT}\phi(\vec{r})\right\} + c_i(\vec{r})\vec{v}(\vec{r}), \tag{1}$$

where $\vec{v}_i, c_i, z_i$, and D_i are, respectively, the velocity, the local concentration (in mol per liter), the valence, and the diffusion coefficient of the ionic species i. The electric potential is represented by means of the symbol ϕ; and $\vec{v}$ is the fluid velocity. The constant e represents the elementary charge, while k and T are, respectively, the Boltzmann constant and the absolute temperature. Note that the correction factor γ_i is known conventionally as the ion activity coefficient accounting for the interactions with other ions and the solvent ($\gamma_i = 1$ for an ideal solution).

In previous works [15,16] we presented this modified model with the aim to identify and clarify the consequences of a single effect, namely the excluded volume of ions, which has a clear physical interpretation: the concentration of ions that builds up at regions of high electric potential cannot exceed a given limiting value mainly determined by the hydration radius, so that the Boltzmann distribution breaks down. Under these conditions, a remarkably simple distribution law can be formulated postulating that the ion concentrations are expressed by a Langmuir-type correction for the excluded volume [22,23],

$$\gamma_i = \frac{1}{1 - \sum_{i=1}^{m} \frac{c_i(\vec{r})}{c_i^{\max}}}, \tag{2}$$

where $c_i^{\max}$ is the maximum local concentration of ionic species i due to the finite ion size.

Here we extend our previous analysis incorporating into the model the physical requirement that the finite ion size also establishes a distance of closest approach of the ions to the particle surface, resulting from ion–particle surface interactions. Therefore, we now assume that ions cannot come closer to the surface of the particle than their effective hydration radius, R (i.e., the ion density is defined only for $r > a + R$, while the electrostatic field is defined for all $r \geqslant a$). It is worth noting that the ion behavior is independent of its charge distribution, as long as it has central symmetry. Therefore, an ion can be represented by a sphere with a point charge at its center, which justifies the condition that this charge cannot come closer to the particle surface than the ion radius.

As usual, the equation system is first linearized with respect to the applied field. The resulting equation system together with the appropriate boundary conditions constitutes the theoretical model considering the excluded volume effect (for further details we refer the reader to Ref. [16]).

3. Results and discussion

The theoretical model can be numerically solved yielding the electric potential and ion concentration profiles as a function of the distance from the surface of the particle. The numerical calculations were performed using the network simulation method [24,25]. The obtained results differ with respect to those presented in [15,16] because we now include the condition that ions cannot come closer to the surface of the particle than their own excluded volume radius. Another difference is that in the comparison of the various profiles calculated for different ion sizes we now keep constant the charge of the particle rather than its surface potential. This way of doing has the advantage of using as parameter a particle property that can be directly measured, rather than a model-dependent property that can only be calculated. It also greatly simplifies the interpretations. The different constant and parameter values used in the calculations, except when specified otherwise, are given in Table 1.

For sake of simplicity we consider a binary univalent electrolyte and assume that $c^{\max}$ has the same value for both ionic species,

$$c^{\max} = \frac{1}{10^3 N_A V}, \tag{3}$$

where V is the average volume occupied by an ion in the solution and N_A is the Avogadro number. The $c^{\max}$ values chosen for the graph, $c^{\max} = 0.2$, 1.5, and 13 M, together with the standard model results, correspond to effective ion radii of approximately 1.0, 0.5, 0.25 nm, and zero. These last values were calculated using Eq. (3) with $V = (2R)^3$, which corresponds to a cubic lattice (52% packing). This $c^{\max}$ set spans the whole range of theoretically possible values since, for $c^{\max} = 0.2$ M (1.0 nm effective radius) and at the chosen $\kappa a = 104$ value, the ion concentration is saturated everywhere: $c^{\infty} = c^{\max}/2$. On the other hand, the $c^{\max} = 13$ M value (0.25 nm

Table 1
Parameter values used in the calculations except when specified otherwise.

Radius of the particle	$a = 100 \times 10^{-9}$ m
Elementary charge	$e = 1.602 \times 10^{-19}$ C
Absolute permittivity	$\varepsilon = 78.54 \cdot \varepsilon_0 = 6.954 \times 10^{-12}$ F m^{-1}
Boltzmann constant	$k = 1.381 \times 10^{-23}$ J/K
Avogadro number	$N_A = 6.022 \times 10^{23}$ mol^{-1}
Temperature	$T = 298$ K
Number of ion species in the solution	2
Ion valences	$z_1 = -z_2 = 1$
Bulk concentration of ionic species	$c_1^{\infty} = c_2^{\infty} = 0.1$ M
Charge of the particle	$Q = 2 \times 10^{-14}$ C
Reciprocal Debye length	$\kappa \approx 10^9$ m^{-1}
Fluid viscosity	$\eta = 0.89 \times 10^{-3}$ P

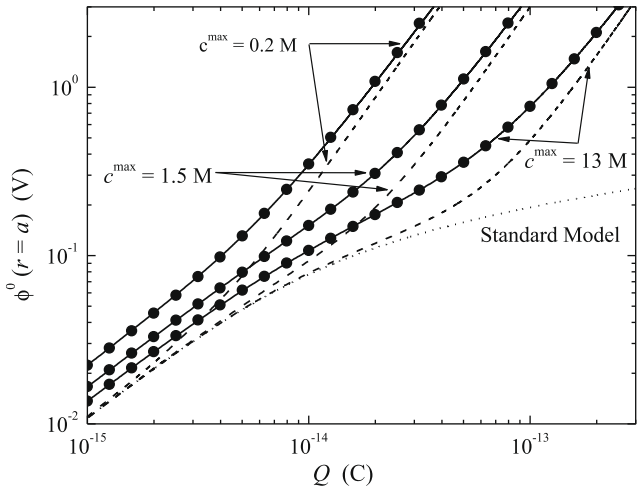

Fig. 1. Surface potential as a function of the fixed charge of the particle, calculated for the indicated c^{max} values. Numerical results obtained using condition $c_i(r < a + R) = 0$ (solid lines), considering that ions can come arbitrarily close to the particle (dash lines), standard model results (dot line), and analytical expression (4) (solid circles). The other parameters are given in Table 1.

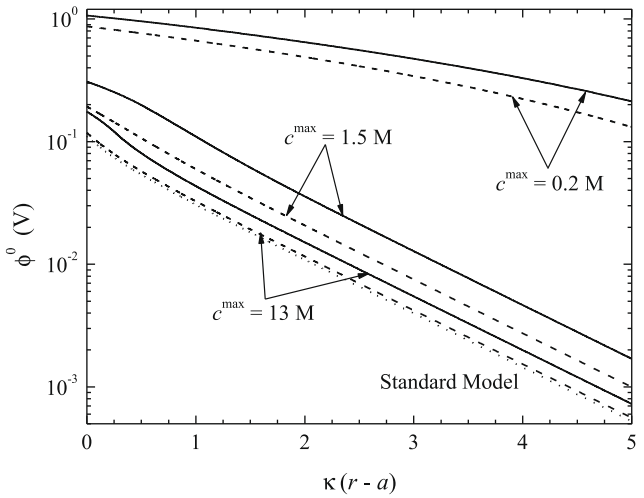

Fig. 2. Equilibrium electric potential profiles calculated for the indicated c^{max} values while keeping constant the fixed charge of the particle. Numerical results obtained using condition c_i $(r < a + R) = 0$ (solid lines), considering that ions can come arbitrarily close to the particle (dash lines), and standard model results (dot line). The other parameters are given in Table 1.

effective radius), should be close to a typical value for a real hydrated ion.

Fig. 1 shows the equilibrium surface potential as a function of the particle charge (solid lines), calculated for the indicated c^{max} values using the theoretical model presented in this work. Also included for comparison are our previous results [15], obtained considering that ions can come arbitrarily close to the particle (dash lines), as well as the standard model results (dot line). The lines with solid circles correspond to the analytical expression

$$\phi^0(a) = \frac{Q}{4\pi\varepsilon a} - \frac{kT\kappa a(a+R)}{ea} \sqrt{\frac{2c^{max}}{\sum_{i=1}^{m} z_i^2 c_i^{\infty}} \ln\left\{1 + \sum_{i=1}^{m} \frac{c_i^{\infty}}{c^{max}}\left[\exp\left(-\frac{z_i e}{kT}\left(\phi^0(a) - \frac{Q}{4\pi\varepsilon a}\frac{R}{a+R}\right)\right) - 1\right]\right\}}, \tag{4}$$

where

$$\kappa = \sqrt{\frac{1000e^2 N_A \sum_{i=1}^{m} z_i^2 c_i^{\infty}}{\varepsilon kT}} \tag{5}$$

is the reciprocal Debye length, which is easily deduced adding the exclusion region near the particle surface in the expression proposed in [15] for the reduced surface charge density. As can be observed, Eq. (4) appears to be a good approximation for all the considered c^{max} values.

For low surface charge values, numerical results obtained taking into account the ion size but considering that ions can come arbitrarily close to the particle coincide with those of the standard model, since ion saturation does not occur. However, higher surface potential values are obtained when the exclusion region near the particle surface is incorporated in the model, since the volume charge of the double layer is shifted further away from the surface.

For high surface charge values, the excluded volume effect leads to surface potential values that are much higher than those predicted by the standard model. As already discussed in [15], this occurs because ion saturation always increases the thickness of the double layer. While the inclusion of the condition that ions cannot come arbitrarily close to the particle surface increases even more the surface potential value, the change with respect to the old boundary condition becomes negligible for very high surface charge values, when the thickness of the saturation zone is much higher than the effective ion radius.

Fig. 2 represents the equilibrium surface potential profiles (solid lines), calculated assuming that ions cannot come closer to the surface of the particle than their hydration radius and keeping constant the surface charge of the particle. Also included for comparison are our previous results [15], obtained considering that ions can come arbitrarily close to the particle (dash lines), as well as the standard model results (dot line).

As expected, the new boundary condition, $c_i(r < a + R) = 0$, always leads to higher equilibrium potential values than the previous condition since the charge density surrounding the particle is moved further from its surface while the total value of this charge remains constant. Fig. 2 also shows that the new boundary condition is particularly important in the case of relatively small ions since, under these conditions, the effect of ion saturation is weak while the effect of the existence of a minimum separation between ions and the surface does not vanish. Because of this same reason, the excluded volume effect becomes nonnegligible even for weakly charged particles.

Fig. 3 shows the equilibrium counterion concentration profiles (solid lines), calculated using the theoretical model presented in this work and keeping constant the surface charge of the particle.

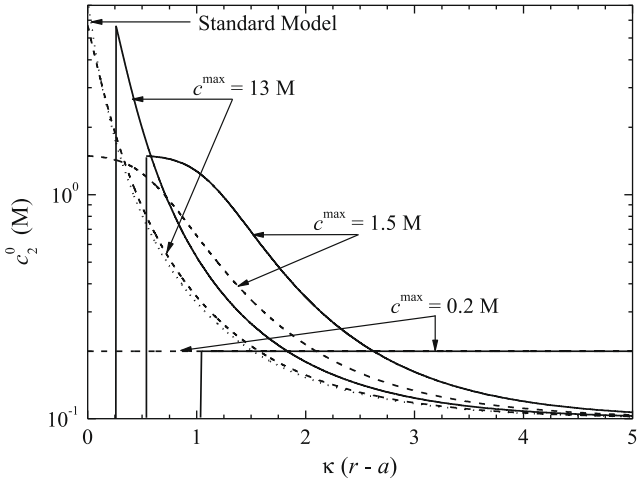

Fig. 3. As for Fig. 2, but calculated for the equilibrium counterion concentration.

Also included for comparison are our previous results [15], obtained considering that ions can come arbitrarily close to the particle (dash lines), as well as the standard model results (dot line).

As expected, the new boundary condition leads to two main changes with respect to the previous condition: the equilibrium concentration values drop to zero at a distance of a hydration radius from the surface and the counterion density extends further away from the particle because the saturation values are not affected. The apparently different behavior of the c^{max} = 0.2 M curve occurs because, as already noted, the ion concentration is saturated everywhere. Therefore, the counterion concentration remains at a constant $c_2^0 \approx c^{max} = 2c^\infty$ value (while $c_1^0 \approx 0$) over a greater distance than plotted in Fig. 3, but eventually drops to the $c_2^0 = c^\infty$ value (while $c_1^0 = c^\infty$) just as the remaining curves.

Close to the particle, at distances for which the counterion concentrations suddenly raise from zero, the equilibrium potentials change from being a solution of the Laplace to a solution of the Poisson equation. This change remains almost imperceptible in Fig. 2 since, for these distances, both the potential and the normal electric field values are continuous. However, the solid and dash curves corresponding to the c^{max} = 13 M exhibit slightly different behaviors close to the particle surface.

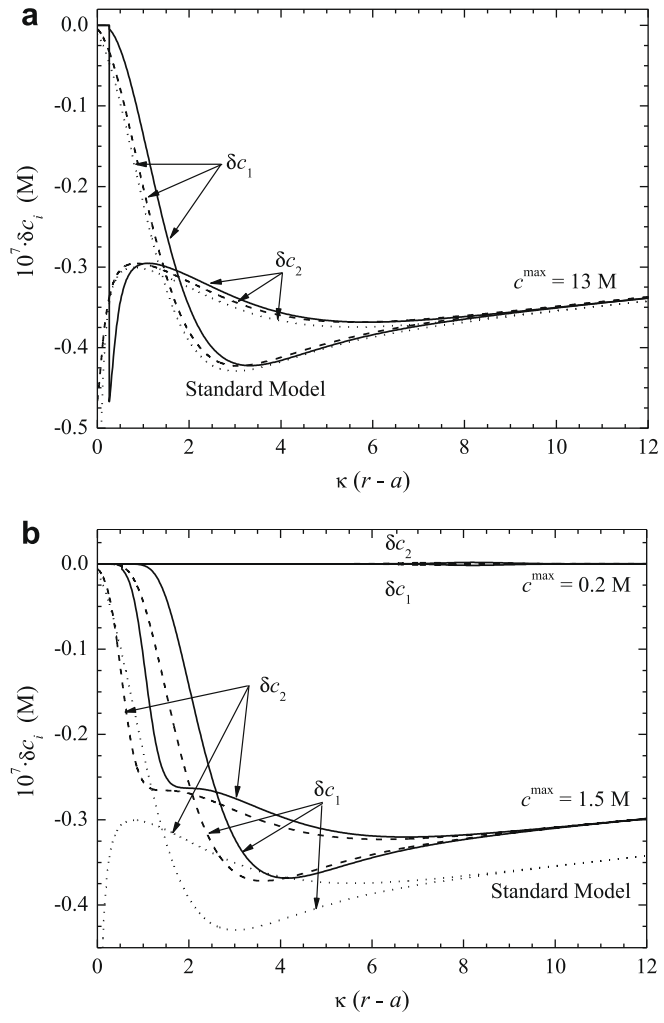

Fig. 4. Field-induced counterion and co-ion concentration change profiles, calculated for the indicated c^{max} values while keeping constant the fixed charge of the particle and assuming that there is no fluid flow: $\eta \to \infty$. Numerical results obtained using condition $c_i(r < a + R) = 0$ (solid lines), considering that ions can come arbitrarily close to the particle (dash lines), and standard model results (dot lines). The other parameters are given in Table 1.

Fig. 4 shows the field-induced counterion and co-ion concentration change profiles calculated considering that there is no fluid convection (the fluid viscosity was set to a very high value: $\eta \to \infty$). It is advisable to examine this limiting situation before the full case where convection is taken into account.

The standard model curves (dot lines) show the familiar behavior characterized by a maximum (in modulus) of the counterion density change on the surface of the particle, then a negative charge density layer, then a positive charge density layer, and finally a broad neutral region of lowered electrolyte concentration [26]. The curves obtained using the old boundary condition (dash lines) differ from this behavior in that both the counterion and the co-ion concentration changes remain equal to zero across the ion saturation zones, as expected. Furthermore, these changes decrease (in modulus) when the ion size increases.

The new boundary condition has a rather weak influence on the ion concentration change curves (solid lines). All the above-noted features remain unaltered except that, additionally, these changes vanish from the surface of the particle to a distance equal to the effective ion radius, as expected.

The qualitatively different behavior of the c^{max} = 0.2 M curves occurs because the ion concentration is saturated everywhere. Therefore, δc_2 for counterions must be equal and opposite to δc_1 for co-ions and no neutral region outside the double layer with a lowered electrolyte concentration is possible. Both effects are clearly visible in Fig. 4.

Fig. 5 represents the tangential flow profile calculated over the particle equator ($\theta = \pi/2$). The curve corresponding to the standard model has the highest slope at the origin because of the extremely high value of the counterion density close to the particle surface (Fig. 3). However, at greater distances, it has the lowest tangential velocity value since all the double layer charge is close to the point where the velocity vanishes due to the adhesion condition.

The curves obtained using the old boundary condition (dash lines) show a strong increase of the tangential velocity far from the particle, which is due to the corresponding increase of the thickness of the double layer (Fig. 3). At constant surface charge, the amount of charge in the double layer is also constant but it is spread out further away from the surface and is located, therefore, at a greater distance from zero velocity boundary.

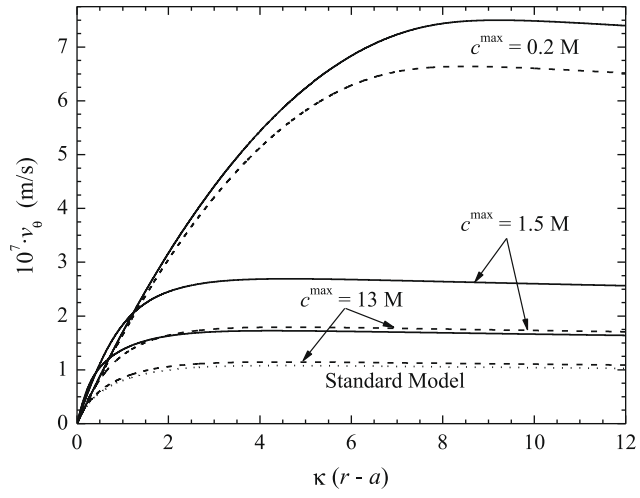

Fig. 5. Tangential fluid velocity profiles, calculated over the particle equator ($\theta = \pi/2$) for the indicated value of c^{max} while keeping constant the fixed charge of the particle. Numerical results obtained using condition $c_i(r < a + R) = 0$ (solid lines), considering that ions can come arbitrarily close to the particle (dash lines), and standard model results (dot line). The other parameters are given in Table 1.

The new boundary condition (solid lines) further increases the fluid velocity value far from the particle, since it moves the double layer charge even further away from the particle surface. However, very close to the surface, the velocity is lower since there is no charge in the first layer with a thickness of one effective ion radius. The overall effect is particularly strong for small ions since, for thick saturation zones, the change due to the new boundary condition becomes relatively unimportant.

It should be noted that for the extreme case c^{max} = 0.2 M, the ion saturation in the whole space does not prevent the fluid flow near the surface which, on the contrary, is particularly strong.

Fig. 6 shows the final results for the field-induced ion concentration change profiles taking convection into account. The standard model curves (dot lines) show that convection increases (in modulus) the concentration changes, as expected.

The curves obtained using the old boundary condition (dash lines) show that the increment of convection with the ion size (Fig. 5) is sufficiently strong as to invert their relative placement: the ion concentration changes increase (in modulus) with the ion size instead of decreasing as in Fig. 4.

The new boundary condition leads to an additional increment of the fluid convection (Fig. 5) which is, furthermore, more significant for the smaller ion sizes. Therefore, the corresponding curves (solid lines) strongly deviate now from those obtained using the old boundary condition for small ions, and less so for bigger ones. This leads to a nonmonotonous behavior in Fig. 6 with the largest amplitude of the lowered electrolyte concentration of the neutral region corresponding to c^{max} = 1.5 M followed by c^{max} = 13 M.

More importantly, Fig. 6 shows that due to fluid convection and the new boundary condition, the field-induced ion concentration changes corresponding to small ions strongly differ from the prediction of the standard model. This contrasts with Figs. 1–3, which only show small differences between the predictions of the standard model and the corresponding results for small ions, obtained using both the old and the new boundary conditions.

Fig. 7 represents the field-induced electric potential change profiles, calculated keeping constant the surface charge of the particle (the straight dash dot line corresponding to the potential of the applied field E is also included). Most notable are the almost constant values of $\delta\phi$ throughout the saturation zones, which occur because the applied field cannot change the ion concentrations in these regions. Therefore, the potential changes inside the saturation zones are only due to concentration changes outside these zones and to the applied potential.

As can be seen, the standard model (dot line) predicts in the considered case a negative dipole coefficient (the corresponding potential curve approaches the applied potential line from below). The curves obtained using the old boundary condition (dash lines) correspond to dipole coefficients that strongly increase with the ion size (the dipolar coefficient is still negative for R = 0.25 nm but becomes positive for R = 0.50 nm and R = 1.0 nm). Going back to Fig. 6, these conclusions show that the dipole moment corresponding to the negative charge density close to the particle is larger than that of the positive charge density further away from the surface in the case of the standard model and for c^{max} = 13 M. However, the opposite is true for c^{max} = 1.5 M and c^{max} = 0.2 M (actually the positive charge density disappears in this last case).

The new boundary condition (solid lines) leads to even larger dipole coefficients as compared to those obtained using the old boundary condition. The differences are specially pronounced for small ions, to the point that even for c^{max} = 13 M the dipole coefficient is already positive.

Fig. 8 represents the conductivity increment ΔK defined as

$$K = K^{\infty}(1 + \varphi\Delta K) = K^{\infty}(1 + 3\varphi d) \tag{6}$$

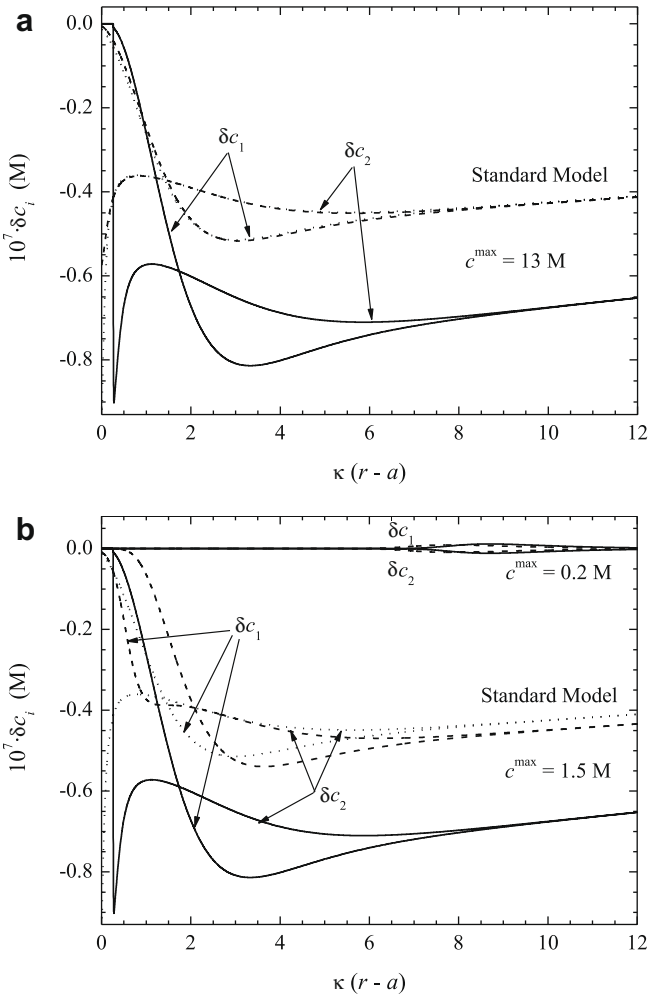

Fig. 6. As for Fig. 4 but including fluid flow.

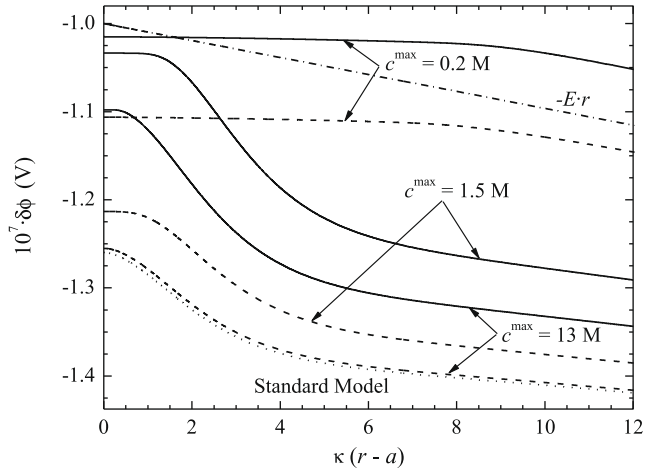

Fig. 7. Field-induced electric potential change profiles, calculated for the indicated c^{max} values while keeping constant the fixed charge of the particle. Numerical results obtained using condition $c_i(r < a + R) = 0$ (solid lines), considering that ions can come arbitrarily close to the particle (dash lines), and standard model results (dot line). The straight (dash dot) line corresponds to the applied potential. The other parameters are given in Table 1.

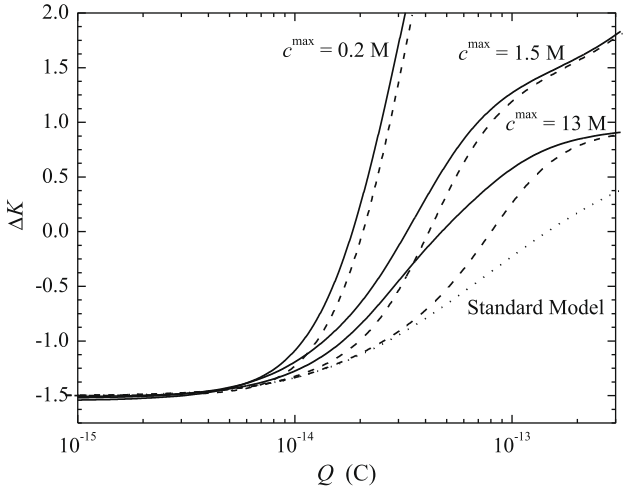

Fig. 8. Conductivity increment ΔK as a function of the fixed charge of the particle, calculated for the indicated c^{max} values. Numerical results obtained using condition $c_i(r < a + R) = 0$ (solid lines), considering that ions can come arbitrarily close to the particle (dash lines), and standard model results (dot line). The other parameters are given in Table 1.

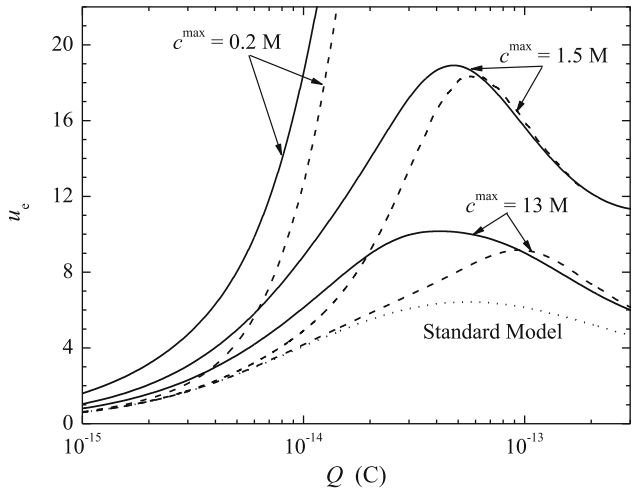

Fig. 9. Dimensionless electrophoretic mobility u_e as a function of the fixed charge of the particle, calculated for the indicated c^{max} values. Numerical results obtained using condition $c_i(r < a + R) = 0$ (solid lines), considering that ions can come arbitrarily close to the particle (dash lines), and standard model results (dot line). The other parameters are given in Table 1.

as a function of the fixed charge of the particle. In this expression K and K^∞ are the conductivities of the suspension and of the suspending medium, respectively, φ is the volume fraction occupied by the particles, and d is the dipolar coefficient.

For very low particle charge values, both the standard model results (dot line) and the results obtained using the old boundary condition (dash lines) converge, as expected, to the value $\Delta K = -3/2$, which corresponds to the dipolar coefficient of an insulating uncharged sphere in a conducting medium $d = -1/2$. As for the results obtained using the new boundary condition (solid lines), they converge to a slightly lower value $\Delta K = -3(a + R)^3/(2a^3)$, since, for $Q = 0$, the new boundary condition basically increments the particle radius by one effective ion radius.

For increasing particle charge values, the standard model results (dot line) also increase tending to the limiting value $\Delta K \approx 3/4$ that corresponds to $d \approx 1/4$ [27,28]. Conductivity increment values obtained using the old boundary condition (dash lines) are always higher than those predicted by the standard model and the difference increases with the ion size. However, strong deviations only occur for high particle charges since they are due to the counterion saturation close to its surface (Fig. 3). On the contrary, the extension of the theoretical model presented in this work leads to conductivity increment values (solid lines) that strongly deviate from the standard model results even for low and medium particle charges, due to the effect of the shift of the double layer one effective ion radius away from the particle surface.

For very high particle charge values, the results obtained using the old and the new boundary conditions coincide with one another: one effective ion radius becomes negligible as compared to the thickness of the counterion saturation zone. This behavior means that both the ion size effect in the suspending medium and the new boundary condition are essential to the model: the low particle charge behavior is mainly determined by the new boundary condition while, for high particle charges, the model behavior is mainly determined by the ion size effect across the double layer. It should finally be noted that the unbounded increase of the conductivity increment with the particle charge is simply due to an increment of the effective particle radius by the thickness of the saturation zone.

Fig. 9 represents the dimensionless electrophoretic mobility defined as

$$u_e = \frac{3e\eta}{2\varepsilon kT}\frac{v_e}{E}$$

as a function of the fixed charge of the particle (in this expression v_e is the electrophoretic velocity). The standard model curve (dot line) shows the familiar nonmonotonous behavior [29] (note, however, the dependence on the particle charge rather than the ζ potential and the logarithmic scale).

The results obtained using the old boundary condition (dash lines) show a substantial increase of the mobility with the ion size [16] due to the increment of the tangential fluid velocity (Fig. 4). However, this increment becomes negligible for small ions and low particle charge values when counterion saturation near the particle surface disappears. On the contrary, the results obtained using the new boundary condition (solid lines) show substantial increments with respect to the standard model even for small ions and low particle charges. This happens because the shift of the double layer one effective ion radius away from the particle surface does not vanish in this case. The predicted behavior opens the possibility for a theoretical interpretation of a series of experimental mobility values that are higher than the maximum allowed by the standard model [30].

4. Conclusion

We extend our previous works that modify the standard electrokinetic model taking into account the finite size of ions in the electrolyte solution. There we considered that the local ion concentration cannot surpass a finite maximum value determined by the ion size. Here we add the requirement that the finite ion size also determines a distance of closest approach of ions to the particle surface. We show that both the ion size effect in the suspending medium and the distance of closest approach are essential to the model: the low particle charge behavior is mainly determined by the latter, while the former mainly determines the model behavior for high particle charges.

While previous works dealing with equilibrium properties conclude that ion size effects are only significant for highly charged particles and high electrolyte concentrations, our nonequilibrium results show that largely due to the above-noted extension of our previous results and to ion convection, these effects are not negligible even for weakly charged particles. Moreover, they

generally improve the predictions of the standard electrokinetic model: both the electrophoretic mobility and the conductivity increment increase. This opens the possibility for a theoretical interpretation of experimental mobility values that are higher than the maximum allowed by the standard electrokinetic model.

We finally wish to stress that the considered modification is fundamentally different from other extensions of the standard electrokinetic model dealing with the particle–electrolyte solution interface. While suspended particles may, or may not, be surrounded by a surface layer with specific properties, it is quite certain that ions in the electrolyte solution do have a finite size. Therefore, the excluded volume effect should have a universal character, even though the way in which the finite ion size is incorporated into the equations may vary. We also note that out treatment does not pretend to address other limitations of the mean field theory such as specific ion–ion interactions and correlations [31], which would require radical changes of the theoretical model.

Acknowledgments

Financial support for this work by MEC (Project FIS2006-4460), FEDER funds, and Junta de Andalucía (Project FQM-410), of Spain; as well as by CIUNT (Projects 26/E312 and 26/E419) and CONICET (PIP 4656) of Argentina, is gratefully acknowledged.

References

[1] R.W. O'Brien, W.T. Perrins, J. Colloid Interface Sci. 99 (1984) 20.
[2] C.F. Zukoski, D.A. Saville, J. Colloid Interface Sci. 107 (1985) 322.
[3] J. Kijlstra, H.P. Van Leeuwen, J. Lyklema, Langmuir 9 (1993) 1625.
[4] D.F. Myers, D.A. Saville, J. Colloid Interface Sci. 131 (1989) 461.
[5] L.A. Rosen, D.A. Saville, Langmuir 7 (1991) 36.
[6] A.V. Delgado, F. González-Caballero, R.J. Hunter, L.K. Koopal, J. Lyklema, J. Colloid Interface Sci. 309 (2007) 194.
[7] T.S. Simonova, V.N. Shilov, Kolloid. Zh. 48 (1986) 370.
[8] C.F. Zukoski, D.A. Saville, J. Colloid Interface Sci. 114 (1986) 32.
[9] C.S. Mangelsdorf, L.R. White, J. Chem. Soc. Faraday Trans. 86 (1990) 2859.
[10] C.S. Mangelsdorf, L.R. White, J. Chem. Soc. Faraday Trans. 94 (1998) 2441.
[11] C.S. Mangelsdorf, L.R. White, J. Chem. Soc. Faraday Trans. 94 (1998) 2583.
[12] J.J. López-García, C. Grosse, J. Horno, J. Phys. Chem. B 111 (2007) 8985.
[13] C.F. Zukoski, D.A. Saville, J. Colloid Interface Sci. 114 (1986) 45.
[14] D.E. Dunstan, J. Colloid Interface Sci. 163 (1994) 255.
[15] J.J. López-García, M.J. Aranda-Rascón, J. Horno, J. Colloid Interface Sci. 316 (2007) 196.
[16] J.J. López-García, M.J. Aranda-Rascón, J. Horno, J. Colloid Interface Sci. 323 (2008) 146.
[17] J.J. Bikerman, Philos. Mag. 33 (1942) 384.
[18] M. Eigen, E. Wicke, J. Phys. Chem. 58 (1954) 702.
[19] S. Levine, G.M. Bell, Discuss. Faraday Soc. 42 (1966) 69.
[20] E. Ruckenstein, D. Schiby, Langmuir 1 (1985) 612.
[21] P. Strating, F.W. Wiegel, Phys. A 193 (1993) 413.
[22] Z. Adamczyk, P. Warszysnky, Adv. Colloid Interface Sci. 63 (1996) 41.
[23] M.S. Kilic, M.Z. Bazant, A. Ajdari, Phys. Rev. E 75 (2007) 021503.
[24] J.J. López-García, J. Horno, A.V. Delgado, F. González-Caballero, J. Phys. Chem. 51 (1999) 103.
[25] J.J. López-García, C. Grosse, J. Horno, J. Colloid Interface Sci. 265 (2003) 327.
[26] S. Pedrosa, C. Grosse, J. Colloid Interface Sci. 219 (1999) 37.
[27] C. Grosse, K. Foster, J. Phys. Chem. 91 (1987) 2073.
[28] C. Grosse, F.J. Arroyo, V. Shilov, A.V. Delgado, J. Colloid Interface Sci. 242 (2001) 75.
[29] R.W. O'Brien, L.R. White, J. Chem. Soc. Faraday Trans. 2 (74) (1978) 1607.
[30] F.J. Arroyo, F. Carrique, A.V. Delgado, J. Colloid Interface Sci. 217 (1999) 411.
[31] J. Lyklema, Fundamentals of Interface and Colloid Science, vol. II, Sect. 3.6a, 3.6b, Academic Press, San Diego, 1995.